IEEE Access
Multidisciplinary | Rapid Review | Open Access Journal

Received October 18, 2019, accepted October 29, 2019, date of publication October 31, 2019, date of current version November 13, 2019.

Digital Object Identifier 10.1109/ACCESS.2019.2950754

Whitelisting in RFDMA Networks

TOMAŽ ŠOLC[1,2], HALIL YETGIN[1,3], TIMOTEJ GALE[1], MIHAEL MOHORČIČ[1,2], (Senior Member, IEEE), AND CAROLINA FORTUNA[1]

[1]Department of Communication Systems, Jožef Stefan Institute, 1000 Ljubljana, Slovenia
[2]Jožef Stefan International Postgraduate School, 1000 Ljubljana, Slovenia
[3]Department of Electrical and Electronics Engineering, Bitlis Eren University, 13000 Bitlis, Turkey

Corresponding author: Halil Yetgin (hyetgin@beu.edu.tr)

This work was supported in part by the Slovenian Research Agency under Grant P2-0016, and in part by the European Community projects, including eWINE under Grant 688116 and NRG-5 under Grant 762013.

ABSTRACT Uplink transmissions, within coexisting distinct sub-GHz technologies operating in the same unlicensed band, can be exposed to detrimental impact of the interference. In such scenarios, transmission scheduling becomes important for mitigating interference or minimizing the impact of the interference. For this purpose, we aim to whitelist relatively better channels in terms of their yielded packet reception ratio using our proposed channel quality metric that is based on the received signal-to-interference-plus-noise ratio. In this paper, we investigate the trade-offs of the channel whitelisting in random frequency division multiple access (RFDMA) networks in the presence of the cumulative intra- and inter-technology interferences. Our main findings indicate that, although channel whitelisting reduces the degree of freedom, and thus the overall capacity, it empowers a certain amount of devices to be served at a much lower received signal power, whereas this is infeasible for non-whitelisting scenarios at larger received signal power, which signifies the energy conservation ability of our proposed whitelisting method. It is experimentally demonstrated, on Sigfox, a particular type of RFDMA network, that non-whitelisting scenarios are not capable of supporting any devices at a received signal power below −118 dBm. Even for lower received signal power, we are able to reduce the required number of retransmissions at the same reception probability, which indeed indicates that the overall reliability of the network is improved.

INDEX TERMS Aloha, inter-technology interference, Internet of things, RFDMA, whitelisting.

I. INTRODUCTION

The coexistence of heterogeneous technologies, particularly in unlicensed or shared license spectrum including sub-GHz is vitally important for multi-user transmissions in order to increase spectral efficiency and overall throughput, while mitigating interference and satisfying predefined quality of service (QoS) requirements [1]. In this context, whitelisting/blacklisting [2] approaches are more traditional candidates for co-existence while non-orthogonal multiple access (NOMA), cooperative NOMA [3], and cognitive radio [4] represent more recent and advanced candidates.

One of the major challenges that has emerged in sub-GHz wireless communication is the allotment of the transmissions medium in a distributed manner, considering that a growing number of sub-GHz technologies are emerging and expected to coexists in that unlicensed band. Existing studies heavily focus on the coexistence of different technologies in the 2.4 GHz and 5 GHz bands [5] and very little is known about the coexistence of different technologies in sub-GHz bands, particularly in terms of the detrimental impact of the interference arriving both from intra- and inter-technology devices, i.e. devices belonging to the same and different technology, respectively [6].

On the other hand, devices lying within the IoT environment usually operate on energy-constrained batteries, where they are inherently capable of sensing, gathering and transmitting data, rather than solely receiving and processing. Therefore, it is vitally important to maximize the lifetime of devices for the sake of prolonged and uninterrupted communications [7]. One of the solutions to minimize the overall energy dissipation is to utilize ultra narrowband (UNB) systems in order to benefit from low power levels and effective long range transmissions. For example, low power wide-area networks (LP-WAN) [8] communication technologies are emerging as the de-facto IoT enablers.

The associate editor coordinating the review of this manuscript and approving it for publication was Gongbo Zhou.

UNB systems enable channels with very narrow bandwidth, typically 100 Hz, which can be around one thousand times narrower than the entire channel bandwidth [9]. However, one inherent issue of UNB is the oscillator imprecision [9], which can lead to inaccuracy in the central frequency that is larger than the channel bandwidth, for instance, while operating at 868 MHz in Europe. Therefore, perfect orthogonal channels may not be applicable to UNB systems and precise oscillators can be unduly expensive for large scale implementations. This naturally leads to random frequency division multiple access (RFDMA) scheme for UNB, which is an ALOHA type scheme allowing each device to transmit its message at any arbitrary time instant with a randomly chosen carrier frequency without relying on the channel state information (CSI).

RFDMA gained popularity particularly in ultra-narrowband systems [10]. The narrow bandwidth used by the wireless systems allows a frequency band to be split into a large number of microchannels. The fact that an RFDMA network does not require neither an accurate real-time clock for timing the transmissions nor an accurate frequency reference for defining the channel of transmission is a significant benefit over other multiple access schemes [10]. Therefore, this scheme can readily enable the conservation of the resources that are normally allocated for the overhead dedicated to the reservation of the radio resources. However, a channel whitelisting mechanism mitigating the interference is still required due to the random access nature of the RFDMA [9].

A. CONTRIBUTIONS

The performance of ALOHA [11] and RFDMA [9] methods in terms of network load and interference between devices of the same technology (intra-technology interference) has been well studied in the literature. However, the overall performance of these networks in the presence of external interference from other wireless technologies (inter-technology interference) is not well investigated. Against this background, we analyze the *trade-offs of whitelisting in RFDMA networks in the presence of the cumulative intra- and inter-technology interferences*.[1] The main contributions of this paper are:

1) THE BENEFIT OF WHITELISTS IN RFDMA NETWORKS

The capacity of an RFDMA network directly depends on the degrees of freedom available to devices to select from, where the degrees of freedom correspond to the number of available time slots multiplied by the number of available microchannels. Therefore, a whitelisting strategy can reduce the degrees of freedom, and hence decline the theoretical capacity of the network.

Contrarily, by excluding the microchannels that are experiencing a significant amount of interference, the overall successful packet reception probability of the base station is expected to increase. Despite of taking the reduced degree of freedom into account, indeed whitelisting enables serving a certain amount of devices at a much lower received signal power compared to non-whitelisting scenarios. One of our major contribution in this treatise is that we theoretically derive the conditions when whitelisting is beneficial considering the cumulative intra- and inter-technology interferences.

2) SIMPLE AND PRACTICAL WHITELISTING METHOD

In scenarios, where intra- and inter-technology interferences are present, a whitelisting method for creating the list of relatively better channels should be employed. As a proof of concept, we employ a simple and practical method that is implementation friendly and works globally. Ideally, a channel quality metric can be assigned to each channel according to which certain amount of best channels can be selected for the whitelist.

3) OTHER MAIN CONTRIBUTIONS

1) We investigate several channel quality metrics and propose a smoother, practical and computationally tractable one. We adopt a channel quality indicator metric based on the packet reception ratio as a function of the received signal-to-interference-plus-noise-ratio (SINR) in order to whitelist considerably better channels. To the extent of knowledge, our whitelisting method is the first attempt to identify considerably better channels for uplink transmissions based on the packet reception ratio as a function of the received SINR considering the cumulative interference both from intra- and inter-technology interference scenarios.
2) This study enables RFDMA system designers to understand the behavior of their network setup in realistic conditions, where we conduct a real-testbed experiment using several devices and a base station. Upon our theoretical contributions, we aim to validate the impact of inter-technology interference on the whitelisting, and thus on the spectral efficiency using empirical data gathered from our measurements.
3) Our study also urges the designers to consider spectrum information in order to avoid interference. Possible approaches for collecting such spectrum information can be obtained by spectrum sensing, radio environment maps or some form of spectrum occupancy database. Inter-technology spectrum brokers could also be developed to enable some forms of the inter-technology coordination [1], [5], [13].

The overall structure of this paper is outlined, as follows. We commence with the comprehensive state-of-the-art literature on RFDMA and whitelisting in Section II. Then, we provide the relevant background on ALOHA, on which RFDMA is based, and on intra- and inter-technology interference in Section III. Section IV theoretically derives the benefits of whitelisting in RFDMA in the presence of intra- and

[1]Part of this technical work was presented in European Conference on Networks and Communications (EuCNC) [12].

inter-technology interferences, Section V introduces our proposed whitelisting method and Section VI investigates a broad range of channel quality metrics and elaborates on our proposed channel quality metric to be utilized for the whitelisting method. Our experimental setup and its results are presented in Section VII. Finally, a discussion on channel coherence is provided in Section VIII for the sake of updating the channel whitelist and closing remarks are given in Section IX.

II. RELATED WORK

Having discussed our motivations on the coexisting heterogeneous technologies and described why RFDMA is beneficial for UNB networks, we now provide a comprehensive state-of-the-art literature review on RFDMA and whitelisting.

A. UNB NETWORKS USING RFDMA

In order to maximize the energy efficiency in end devices, the communication protocols should *minimize signaling and overheads*, *minimize retransmissions* and allow *high spectral efficiency*. Random multiple access schemes provide beneficial trade-offs in many use cases. For example, they enable significantly reduced congestion, considering sub-GHz spectrum is getting crowded [1] with the sub-GHz technologies that are being promoted simultaneously, such as LoRa, Sigfox [14], low-rate wireless personal area networks (LR-WPANs), Wi-Fi HaLow and so on. A signaling-free random multiple access scheme is ALOHA, which has already been widely analyzed in the literature [11]. Devices in a typical ALOHA network share the same channel. When a device has a frame of data to transmit through the network, it chooses an arbitrary time for transmission, regardless of any existing radio traffic. Protocols that are based on ALOHA operate well, but only when the number of concurrent contending devices and the overall traffic load are low [15], [16].

Random frequency division multiple access (RFDMA) is an extension of the original ALOHA concept. In traditional ALOHA, the devices randomly choose only the time of transmission. RFDMA expands on this concept by giving devices a large number of frequency channels to arbitrarily select from, in addition to the time of transmission. Similarly to pure and slotted ALOHA versions, transmission frequency in RFDMA can be selected from a continuous range or from a limited number of discrete values [10]. For example, Do *et al.* [10] theoretically analyze the performance of a UNB network with a star topology and a random frequency and time selection technique based on the Sigfox deployment. They consider random frequency selection both from a discrete set and a continuous range, and discuss the effect of tolerances in the transmitter frequency reference. Similarly, Do *et al.* investigate the intra-technology interference effect on the RFDMA performance in terms of outage probability and bit error rate. Moreover, Mo *et al.* [17] analyze the effect of the redundancy-based frame repetitions on the packet loss in a UNB network using random frequency and time multiple access (RFTMA),[2] where they aim to optimize the number of replications (multiple copies of the same payload) to be transmitted in the presence of intra-technology interference. More explicitly, it has been shown in [17] that in most cases collision avoidance allows for greater throughput particularly in congested networks. Additionally, the uplink transmissions of a UNB network along with the overall network capacity and the intra-technology interference in the presence of path-loss and Rayleigh fading are theoretically examined by Mo *et al.* [18]. Most of these existing works on UNB systems using RFDMA focus on the intra-technology interference and tend to be mostly theoretical in nature, whereas we theoretically analyze the benefits of whitelisting and propose a channel whitelisting method considering cumulative intra- and inter-technology interferences realized with the empirical data observed from our measurements.

B. WHITELISTING METHODS

Whitelisting methods mainly constrain wireless devices to only transmit through channels that are usually favorable regarding quality [2], [19], especially when inter-technology interference dominates within the range of uplink transmissions. The motivation of whitelisting is to create a subset of less noisy channels for the sake of better reception of the packets. However, since we consider random selection of the transmission channel and the time-slot, there is a chance of collision, when packets are sent at the same time-slot and through the same transmission channel. Yet, co-channel interference plays a significant role in the overall performance of the networks, when the data transmission is scheduled at the same time-slot through adjacent channels. Therefore, the consideration of interference arriving from both the same and other coexisting technologies must be incorporated into the whitelisting method. For example, one of the earliest studies on whitelisting is conducted by Watteyne *et al.* [19], where they conclude that whitelisting on a link-by-link basis can further improve the connectivity and reliability of the network.

Jeon and Chung [20] focus their attention on the energy minimization of multi-hop networks using enhanced time-slotted channel hopping (ETSCH) based on the proposed adaptive channel quality estimation (A-CQE) method, where ETSCH exploits a non-intrusive channel-quality estimation (NICE) technique [2] for whitelisting that is gleaned by the energy detection of the idle period of each time-slot. This method particularly adopts the interference fluctuations for the channel quality metric, whereas we consider a global whitelist of channels incorporating the effect of intra- and inter-technology interferences. Additionally, Kotsiou *et al.* [21] focus more on the collision avoidance than the impact of external interference. Their main strategy is to group links to assign a particular whitelist so that there

[2]RFDMA is also referred to as RFTMA in the literature. Generally speaking, a few other multiple access schemes using *random frequency and time hopping* technique can also be considered as RFDMA.

is no common frequency band to transmit, which indeed guarantees a collision-free packet transmission. Conversely, we pay attention to intra- and inter- technology interferences focusing on RFDMA networks while determining our global whitelist, which incorporates the effect of interference and ranks the relatively better channels in order. This indeed helps for eliminating the worst channels that are exposed to large amount of interference, particularly due to the inter-technology interference. We elaborate on our whitelisting method in Section V.

III. BACKGROUND

A. ALOHA

In this section, we assume a pure ALOHA system with blind frame repetitions. For each packet of data, a device transmits N_f identical frames, at random times. If at least one frame of N_f is received without error by the base station, the packet is considered to be successfully received. The probability of packet reception p_{rx} can then be calculated as follows [22]:

$$p_{rx} = 1 - (1 - p_f)^{N_f}, \tag{1}$$

where p_f is probability of successfully receiving one frame. If we further assume that frame loss is only affected by collisions within the network, e.g. no external interference, each frame collision results in loss of the corresponding frame considering all devices share a single collision domain. This means if a frame from each device can collide with a frame from any other device, then p_f can be expressed as [22]:

$$p_f = e^{-2G}, \tag{2}$$

where G is total network load and is expressed as the normalized frame transmission rate, which is more explicitly the mean number of frame transmissions across all devices per frame duration. If N_{dev} devices share the collision domain, then G can be expressed as [22]:

$$G = R_{tx} N_f N_{dev}, \tag{3}$$

where R_{tx} is normalized frame transmission rate for an individual device.

In this simplified model, the number of devices which a base station can support for a given fixed p_{rx} is denoted by N_{dev}. In Fig. 1, N_{dev} is plotted versus number of blind frame retransmissions N_f. More explicitly, Fig. 1 illustrates the number of frame repetitions required for attaining a certain packet reception probability within the coverage of a base station containing N_{dev} number of devices. Plausible logic dictates that in order to support a large number of devices within a base station, it is expected that the number of frame repetitions should be increased to satisfy the QoS, which in this case, is defined as the reception probability of 99%. On the contrary, Fig. 1 reveals that a base station can only support a limited amount of devices in order to achieve the predefined packet reception probability and, increasing the number of frame repetitions, for example beyond 6 frames, does not further aid in increasing the number of devices

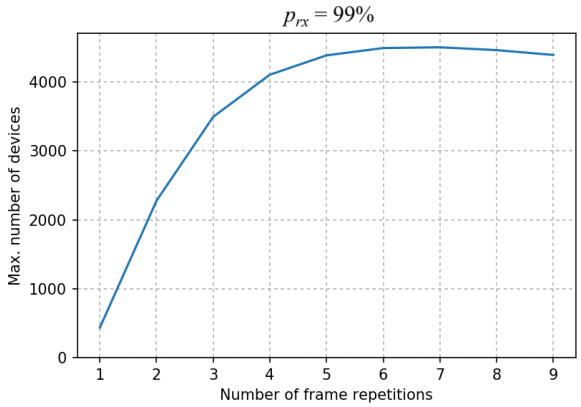

FIGURE 1. Maximum number of devices served by a base station for a minimum QoS defined by p_{rx} versus the number of blind frame repetitions.

that can be supported. This is mainly due to the tremendously increased network load G, to which the number of frame repetitions is linearly proportional, as readily seen in Eq. (3). Indeed, the interesting observation here is that the frame retransmissions, up to a certain point, and without external interference, increase the capacity of the network. A more sophisticated analysis is performed in [17], taking into account channel propagation models, receiver capture, etc. Their simulations show that 3 retransmissions provide a good practical network capacity. The above analysis of Fig. 1 demonstrates that the choice of 6 retransmissions [17] can provide a near-optimal number of devices that can be supported at the QoS defined without the consideration of external interference.

B. INTRA- AND INTER-TECHNOLOGY INTERFERENCE IN RFDMA

From the capacity point of view, a single base station is expected to serve a relatively high number of devices within its transmission range in an IoT network. For instance, in Fig. 2, a Sigfox base station may serve thousands of nodes. The Sigfox protocol is an instance of communication technology that uses RFDMA and is optimized to support concurrent uplink transmissions in order to address the challenges of IoT, e.g., high scalability for handling massive number of devices, wide coverage, low cost and low energy dissipation. Following the ALOHA scheme, each device can transmit its message at any arbitrary time instant with a randomly chosen carrier frequency therefore the higher the number of Sigfox devices the more likely they interfere with each other - leading to intra-technology interference as exemplified in time slot TS-1 of Fig. 2. Intra-technology interference is induced by the density of the same type of technology devices within the network, which can lead to high collision rates particularly for transmission schemes using random access, as explicitly portrayed in Fig. 2. Therefore, in these type of networks, e.g. RFDMA networks, an increase of frame repetitions may be required to compensate packet losses, which can indeed lead to a large amount of energy dissipation.

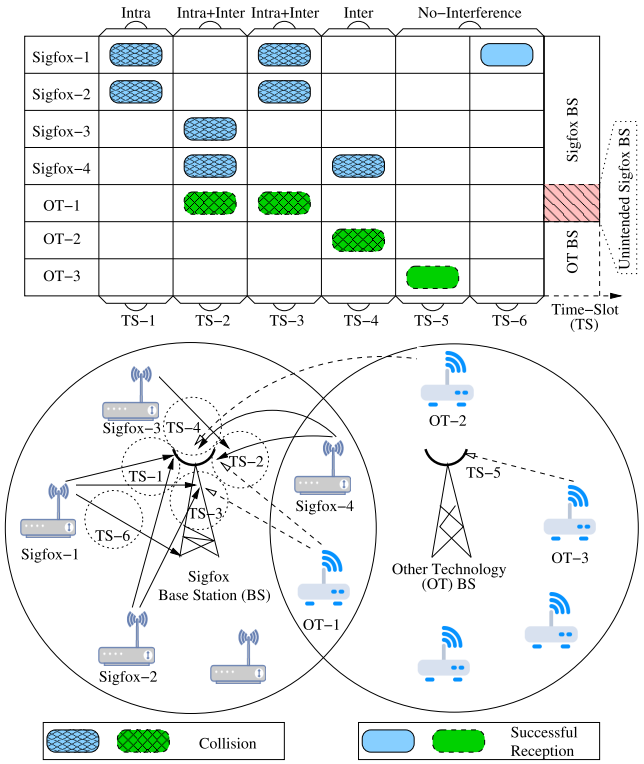

FIGURE 2. The exemplifying illustration of the intra- and inter-technology interferences within an ALOHA-based RFDMA network, assuming that each device transmitting at the same arbitrary time-slot coincides with the same pseudo-randomly selected frequency channel.

Overlapping with the Sigfox channels in the unlicensed 868 MHz, other technologies such as LoRa, IEEE 802.15.4 and proprietary also operate [23] and thus can interfere with the Sigfox network as exemplified in time slot TS-4 of Fig. 2. We refer to inter-technology interference as the interference that arrives from devices that use other communication technologies and share the same frequency bands. In order to be able to eliminate inter-technology interference, spectrum sensing techniques, radio environment maps and spectrum occupancy databases can be leveraged by means of having the global knowledge of the spectrum within the target environment. Inter-technology interference coordination is therefore vitally important for deploying interference-free networks [5].

In real-life scenarios, cumulative interferences arriving both from intra- and inter-technology devices occur. Suppose that the devices are assigned with the same arbitrary transmission channels for the second time-slot (TS-2) of Fig. 2. The illustration shows the cumulative interference coming from the third and the forth Sigfox devices (*Sigfox-3 and Sigfox-4*) described as the intra-technology interference, as well as from the first other technology (OT-1) device depicted as the inter-technology interference (*Intra* + *Inter*). Generally speaking, various options of collisions due to intra- and inter-technology interferences, and successful packet transmissions of an ALOHA-based RFDMA network can be observed in Fig. 2.

IV. THE BENEFIT OF WHITELISTS IN RFDMA NETWORKS

The simple ALOHA model summarized in Section III-A can be extended to an RFDMA network by considering each frequency channel as a separate ALOHA network. In the case of random selection of a transmission channel, the network load is simply divided by the number of available channels N_c, as follows:

$$G' = R_{tx} N_f N_{dev} \frac{1}{N_c}. \tag{4}$$

Hence, the observation regarding the relation between the number of frame repetitions and network capacity still holds. Noting that we assume independent and identically distributed channels.

In realistic scenarios, neighboring channels will interfere, as quantitatively demonstrated in [10]. Let us consider the effect of the interference within the model of [10]. As expected, interference will further decrease the probability of frame reception p_f below the probability that is solely determined by frame collisions. We can model this by introducing the mean probability of packet loss p_i due to interference across all RFDMA channels. Then, modified p_f can be derived as follows:

$$p'_f = (1 - p_i)e^{-2G}, \tag{5}$$

where we can see that large value of p_i has a detrimental effect on the network capacity. Conversely, Eq. (4) indicates that increased N_c has an aiding effect, since the concurrent multiple uplink transmissions enable overall increased capacity. Naturally, these two equations are conflicting, where creating a whitelist of channels induces N_c number of available channels to be effectively decreasing. On the other hand, by optimally selecting channels for the whitelist, the impact of p_i should be significantly diminished. We assume that the more selective we are, the smaller the number of channels for random selection of frequency and time-slots and thus we can obtain a lower p_i. Therefore, whitelisting can be beneficial to improve the overall reliability of the network. Formally derived that the overall reliability of the network can only be improved if the following condition is satisfied, in which Fig. 3 illustrates the plot of Eq. (6):

$$p_i(N_c) < 1 - p'_{f0} e^{2R_{tx} N_f N_{dev} \frac{1}{N_c}}, \tag{6}$$

where p'_{f0} is the probability of frame reception without whitelisting.

Fig. 3 portrays several characteristic values of p'_{f0}, shown as a function of p'_{i0} - initial probability of packet loss (potentially assuming due to interference without whitelisting). The shaded area shows the required range for the $p_i(N_c)$ function for the whitelisting to result in an improved network reliability. By narrowing down the number of available channels N_c, lower probability of packet loss can be achieved, which indeed supports the idea of why the whitelisting is required. The better the whitelisting algorithm, the lower the $p_i(N_c)$ that can be attained. More explicitly, in Fig. 3, outer left hand side (blue colored) area covers the entire available

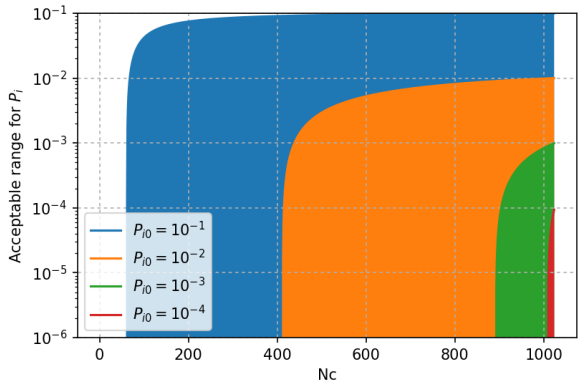

FIGURE 3. The benefit of whitelisting is demonstrated by $p_i(N_c)$, narrowing down the available number of channels and leading to lower probability for packet loss, which in turn improves the reliability of the network.

number of channels, while it can maintain higher packet loss probability of 10^{-1} to 10^{-2}. However, through the inner right hand side (red colored area), the number of available channels are significantly reduced and it can maintain much lower packet loss probability of 10^{-4} to 10^{-6}. Another interpretation of Fig. 3 can be made by following the exponential line of 10^{-2} through approximately 400 number of available channels, which narrows down almost 600 number of available channels and a steep decline to 10^{-6} can be observed in the probability of packet loss.

V. PROPOSED WHITELISTING METHOD

Determining the channels to be whitelisted is a significant challenge, especially when the probability of a collision is large due to massive amount of devices transmitting within the same frequency range. Unlike the well-developed whitelisting methods proposed in [21] and [24] (a complementary concept of blacklisting), which can guarantee collision avoidance, we provide a simple global-whitelisting method with the focus of the impact of the cumulative interference arriving both from intra- and inter-technology devices. Our proposed method, however, can eliminate channels that are exposed to huge amount of interference owing to the channel quality metric proposed in Section VI-D and using the whitelisting procedures described in the following. Note that our intent is not to provide a comparison of whitelisting methods, but rather to inform the designers that whitelisting methods can improve the reliability of an RFDMA network and enable low-power communication in the presence of cumulative intra- and inter-technology interference. Besides, the ratio of the reliability improvement is strictly dependent on the best channels to be utilized, which indeed leads us to the whitelisting method, described as follows.

1) Upon having the measurements data for all available channels and time-slots in an RFDMA network, performed by a spectrum sensor collocated with or integrated in a base station, the quality of a particular channel is averaged over the time-slots it has been used for. For the sake of simplicity, we provide Fig. 4 in order to show how the channels are quantified according to their quality. For example, channel 4 (CH-4) and CH-5 are exemplified using $\overline{PRR}$ function in Eq. 17 of Section VI-D.
2) Then, once all the channels are quantified in terms of their quality, they are arranged in the descending order of quality. For simplicity, we portrayed this procedure in the right bottom side of Fig. 4.
3) From the pool of quality-ordered channels, the whitelist is formed with the method of percentage of

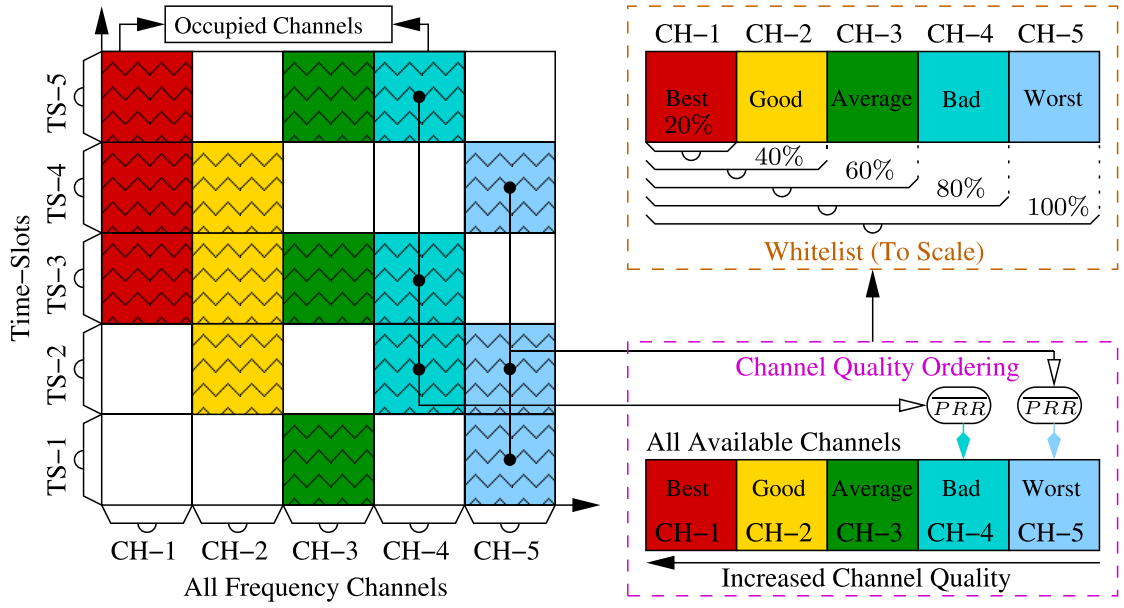

FIGURE 4. An example of RFDMA scheme exhibiting whitelisting method and channel quality ordering based on $\overline{PRR}$ of Eq. (17).

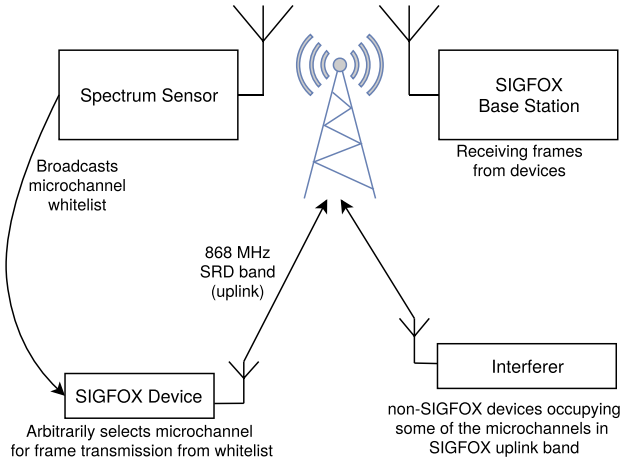

FIGURE 5. The structure overview of the transmission scheme using whitelisting method.

all channels. In our analyses, we select the best "1%, 5%, 10%, 50% and 100%" of all available channels to reveal the benefit of whitelisting.

4) For each scenario of whitelisting using the above-mentioned percentages, the corresponding global whitelist containing relatively better channels are transmitted by the spectrum sensor to every devices within the RFDMA network, as illustrated in Fig. 5.

We strongly believe that using whitelisting with percentages is a simple and effective method for revealing the impact of whitelisting on the performance of the proposed RFDMA network. Suppose that the whitelisting percentages considered in our analyses (1%, 5%, 10%, 50% and 100%) are represented by the percentages portrayed at the top right-side of Fig. 4, which are arranged for five quality-ordered channels, i.e., CH-1, CH-2, CH-3, CH-4 and CH-5 corresponding to "20%, 40%, 60%, 80% and 100%" of all available channels. Statistically speaking by referring to the simple illustration in Fig. 4 that top 20% of all available channels corresponds to CH-1, which in our case, is the "best" quality channel considering 1 out of 5 channels are selected from the quality-ordered list of channels. Top 40% of all available channels corresponds to CH-1 plus CH-2, which are only constituted by the "best" and the "good" quality channels considering 2 out of 5 channels are selected for transmission. We believe that whitelisting percentage approach constrains the transmissions to a limited quality range of channels depending on the amount of percentage in order to allow us to reveal the effect of the whitelisting method on the performance of RFDMA network, as readily observed in Fig. 4.

Nonetheless, due to the dynamic nature of the network, these whitelists are required to be regularly updated. Therefore, one plausible question would be that how frequently the channels within whitelists have to be updated over the base station and circulated through the devices of the RFDMA network? To find the answer to this question, readers are referred to our discussions on channel coherence in Section VIII.

VI. CHANNEL QUALITY METRICS FOR WHITELISTING

While there are a number of channel quality estimators proposed in the literature [25]–[28], they mostly focus on downlink link estimation techniques using a relatively small number of channels. In our scenario, we are particularly interested in a simple and efficient channel estimator that can provide a reliable prediction for packet loss based on the measurement history of the received signal strength indicator (RSSI) from spectrum sensor rather than from packet data information. An alternative approach would be to base the channel quality metric on the prior packet loss statistics for individual channels. For example, a link quality indicator based on packet delivery ratio is proposed by Kotsiou *et al.* [29], but in the absence of external interference. However, this approach is often impractical, since a large number of packets must be transmitted before a reliable statistic per channel can be gathered. This is a vitally important problem considering a large number of microchannels may exist in a typical RFDMA ultra narrowband network and thus the number of packets transmitted per channel may be relatively low. Naturally, this approach requires a large number of packets to be lost before a channel is recognized as unfavorable, which may not be compatible with the QoS requirements.

Nonetheless, Gunatilaka *et al.* [30] demonstrated that channel selection is an important task and using more channels is not always desirable. Therefore, the number of channels to be selected for the whitelist have to be carefully considered within an RFDMA network, particularly due to its random selection nature of the time and frequency slots. Having discussed our general whitelisting method in Section V without detailing the channel selection strategy, we now focus our attention on the development of our own channel quality metric to identify better channels to be selected for the whitelist. In order to achieve this goal, we review several existing channel quality metrics and propose an improved metric in the interest of supporting whitelisting method with the channel selection strategy, where the procedures of channel selection/ordering can be observed in Fig. 4.

A. MEAN CHANNEL AVAILABILITY

One simple channel quality (CQ) metric that is considered for the development of our own channel quality indicator is the mean channel availability (MCA). It is defined as the percentage of time duration, where the interference power in a channel is below a predefined threshold P_{thr}. Suppose our spectrum sensor samples the channel power P_i at times t_i, $i \in [1, 2, 3, \ldots, N]$, this metric then can be defined as follows:

$$MCA = \frac{1}{N} \sum_{i=i_0}^{i_0+N} s_i, \tag{7}$$

where

$$s_i = \begin{cases} 0, & \text{if } P_i < P_{thr}, \\ 1, & \text{otherwise.} \end{cases} \quad \text{and } P_{thr} = P_{rx} - SINR_{min}. \tag{8}$$

P_{rx} denotes the power of the received signal from devices at the base station and $SINR_{min}$[dB] stands for the minimum SINR at which the base station is able to receive the signal, where N is the number of channel power samples from spectrum sensor. However, this metric is controversial, since it assumes a sharp threshold of SINR upon reception. More explicitly, it assumes that 100% of the packets will be lost if interference is above a certain threshold and 0% packet will be lost, otherwise. In realistic applications, the packet loss more or less slowly transitions between these two extremes, as SINR deteriorates.

B. MEAN SIGNAL POWER

A metric that attempts to address the shortcomings of MCA is the mean signal power (MSP) over a time window, defined as follows:

$$MSP = \frac{1}{N} \sum_{i=i_0}^{i_0+N} P_i. \tag{9}$$

A known problem with MSP metric is that it does not take into account the time distribution of interference. Consider a channel where a single strong interferer very occasionally transmits and a channel where a weak interferer transmits continuously. The MSP metric may consider both of these channels identical due to averaging the channel power over the number of channel power samples, N. However, the first channel is expected to have lower packet loss since the probability that a packet in the network will collide with the infrequent interferer is very low. On the contrary, the second channel is expected to continuously lose packets due to constant exposure to interference.

C. TIME AWARE CHANNEL QUALITY

A metric that attempts to consider time distribution of interference is the $CQ(\tau)$ metric [27], referred to as the time-aware channel quality metric, which is defined as follows:

$$CQ(\tau) = \frac{1}{(n-1)} \sum_{j|(j-1)\delta>\tau} j^{(1+\beta)} m_j, \tag{10}$$

where n is the number of samples in a time window at which the metric is calculated and m_j denotes the number of opportunities for which the channel is vacant during j consecutive samples. The metric considers a channel to be vacant, when the measured power of the channel is below P_{thr} threshold, as shown in Eq. (8). Channel power sampling period is depicted by δ, whereas τ stands for the time duration of the packet being transmitted. Hence, jm_j is the total number of channel power samples that appear during the vacancies of length j. The metric sums up all opportunities when their length $(j-1)\delta$ is longer than τ. Eventually, the number of opportunities is divided by the total number of samples (n) during the time window considered. Noda *et al.* [27] introduce an additional parameter β, which determines the bias of the metric towards the channels that have longer transmit opportunities. More explicitly, higher β values promote the selection of channels with larger channel vacancies.

D. AN ADAPTIVE CHANNEL QUALITY METRIC BASED ON ML ESTIMATION

In this study, we introduce a CQ metric based on the maximum likelihood (ML) estimation, referred to as $\overline{PRR}$, which estimates the probability of successful transmission of a packet with length τ. Therefore, a measure of the channel quality based on ML (CQ_ML), the total number of transmission opportunities, depicted as n_{total} and the number of transmission opportunities that do not encounter interference stronger than P_{thr}, denoted by n_{clear}, can be calculated as follows:

$$CQ\_ML = \frac{n_{clear}}{n_{total}}. \tag{11}$$

The total number of transmission opportunities depends on the length of the observed time window (corresponding to n number of samples observed during this time window) and the length of the transmitted packet in samples τ/δ:

$$n_{total} = (n - \tau/\delta). \tag{12}$$

The number of transmission opportunities with no interference can be written as follows (using the same variables as in Eq. (10):

$$n_{clear} = \sum_{j|(j-1)\delta>\tau} (j - \tau/\delta) m_j. \tag{13}$$

Since computing the CQ_ML requires the same variables as computing the previously discussed $CQ(\tau)$ metric and does not necessitate the β parameter, we may refer to it as a simplified channel quality metric, which can be derived as follows:

$$CQ^*(\tau) = \frac{1}{(n - \tau/\delta)} \sum_{j|(j-1)\delta>\tau} (j - \tau/\delta) m_j. \tag{14}$$

However, the simplified channel quality metric CQ^* does not take into account the probability of successful frame reception varying with SINR. Therefore, the proposed ML channel quality estimator can be manipulated with the following method, so that the variation with SINR can be attained. Provided with the recorded history of interference power measurements for a channel, we can estimate the mean interference power $\overline{(P_{int})}_{i_0}$ over the duration of a hypothetical packet transmission starting at sample i_0 of the time instant t_{i_0}, as follows:

$$\overline{(P_{int})}_{i_0} = \frac{1}{\tau/\delta} \sum_{i=i_0}^{i_0+\tau/\delta} (P_{int})_i, \tag{15}$$

where $(P_{int})_i$ is measured interference power in the channel at time instant t_i. Then, hypothetical received $SINR$ at time instant t_{i_0} can be approximated by:

$$SINR_{i_0} = \frac{P_{rx}}{\overline{(P_{int})}_{i_0}}. \tag{16}$$

Supposing that we know the packet reception ratio (PRR) as a function of *SINR*, we can calculate the predicted mean $\overline{PRR}$ of a channel by averaging the calculated *PRR* values for all possible packet transmissions starting at sample i_0 of the time instant t_{i_0}, as follows:

$$\overline{PRR} = \frac{1}{(n-\tau/\delta)} \sum_{i_0=0}^{n-\tau/\delta} PRR(SINR_{i_0}). \tag{17}$$

Consequently, $\overline{PRR}$ of Eq. (17), as a function of the received *SINR*, can aid us with the identification of relatively better channels to be included in our global whitelist, as readily seen in the ''channel quality ordering'' part of Fig. 4.

VII. EXPERIMENTAL SETUP AND RESULTS

The high-level system architecture making use of our proposal to improve the performance of an RFDMA network is illustrated in Fig. 5. We consider a scenario, where an RFDMA uplink band is commonly shared with some other technology devices generating inter-technology interference, in addition to the intra-technology interference. These devices generate interference on some microchannels leading to a lower probability that a frame sent from a device will be successfully received by the base station. Such interfering devices are commonly deployed in practice, for example an unlicensed European SRD band at 868 MHz is utilized for the uplink transmissions.

In our whitelisting proposal, the spectrum sensor in the base station monitors the uplink band and creates a list of microchannels that have the least amount of interference. This list is a whitelist of all microchannels available to devices for the uplink transmissions. The base station periodically broadcasts this list to the devices, using the existing downlink capability of the network. We use a single global whitelist for all devices within a single base station. When the devices are arbitrarily scheduled to transmit, they select a random transmission microchannel from the whitelist, where potentially the impact of interference is mitigated up to a certain level. More technical details about the experimental set-up are provided in [6], and the code[3] as well as the datasets[4] that we were able to release under an open source license are available on GitHub.

A. EMPIRICAL DATA

The experiment was conducted in the 868.130 MHz band. The Sigfox device was programmed to send a total of 1600 packets. In order to measure signal-to-noise ratio (SNR) of the packets, transmitters vary the transmit power by randomly changing the baseband gain from −50 to −20 dB. This range was chosen empirically to cover the entire range of PRR, from 0 to 100%. For each transmitted packet the Sigfox device recorded the transmission time based on the device clock, central frequency in Hz for each frame, amplifier gain or attenuation in dB and the number of frame repetitions were recorded. The Sigfox base station provided measurements related to the physical layer on the receiver end, for example, received time based on base station clock, received signal strength indicator (RSSI) in dBm and SNR in dB (both current packet SNR and average over last 25 packets).

Since multiple clocks and frequency references were used in the system, measurements from all sources needed to be translated onto a common reference in order to present a consistent picture. The offset between device and base station clocks was determined by matching individual packet records through sequence numbers. We ignored the time-of-flight delay. The offset between clocks and frequency references in the test device and the spectrum sensor was determined by matching transmission times and frequencies with the corresponding peaks in the power spectral density. The experimental set-up and the implementation details are similar to those used in [6], which utilizes elements of the Fed4FIRE+ LOG-a-TEC[5] testbed [31].

B. ESTIMATING PRR(SINR)

In Eq. (17), we require PRR as a function of the SINR at the base station. Normally, the impact of channel impairments, such as shadowing effect, Doppler effect, fading, inter-symbol interference and noise at the physical layer can be analytically modeled. Instead, we assume the incorporation of some of these effects, such as noise and interference, into our PRR as a function of SINR, since we actually rely on the empirical measurements of PRR and our proposed network is stationary. Therefore, for computation purposes it is desirable to use the PRR(SINR) function for a real ultra-narrowband receiver. In this section, we describe our methodology to measure the PRR as a function of SINR for the sake of our experimental setup.

The experiment is composed of the transmission of 1600 packets from each indoor transmitter to a single outdoor ultra-narrowband base station. USRP N200 devices are utilized for the uplink transmissions. All packets are transmitted through the channels that are selected amongst 1500 microchannels, each of which is allotted with 100 Hz bandwidth. This channel selection strategy is determined by our proposed whitelisting method, which is based on an adaptive channel quality metric using PRR as a function of the SINR. Devices conduct a frequency hopping operation for an arbitrary time slot.

On the base station side we simultaneously recorded the power spectral density of the base station antenna in the form of RSSI samples for all uplink channels and the received packets. Based on the sequence numbers of the packets we matched the received packets with transmitted ones and marked the transmitted packets that are not successfully

[3]https://github.com/sensorlab/sigfox-toolbox
[4]https://github.com/sensorlab/sigfox-packet-datasets
[5]http://log-a-tec.eu/mtc

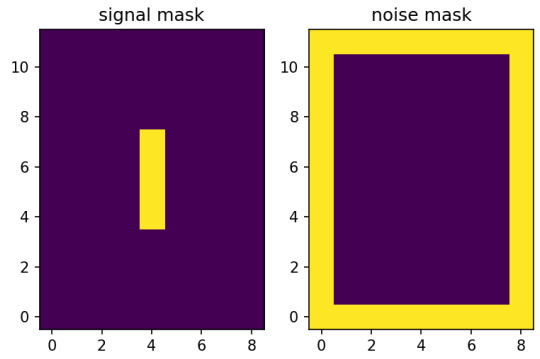

FIGURE 6. Masks used for estimating signal and interference plus noise power from RSSI recordings. Frequency and time domains are situated on the horizontal and vertical axes, respectively. Yellow color corresponds to '1', whereas purple indicates '0'.

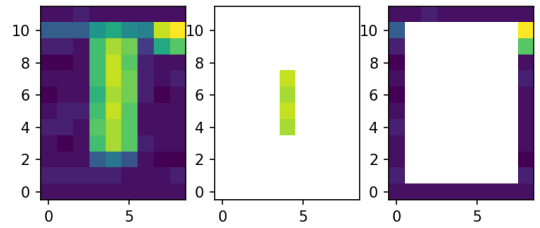

FIGURE 7. Application of masks to spectrum recordings for a single transmission; left-hand side: unmasked RSSI recording, middle: masked data for signal, right-hand side: masked data for noise plus interference.

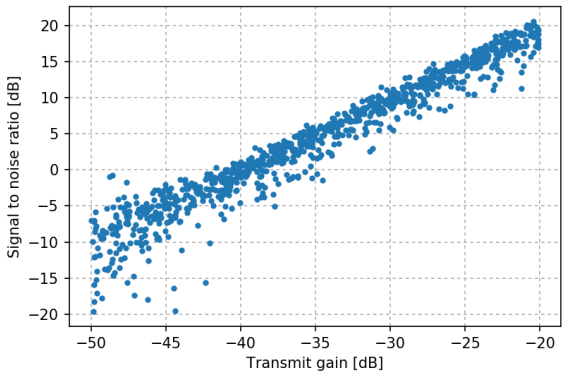

FIGURE 8. Estimated SINR versus transmit gain.

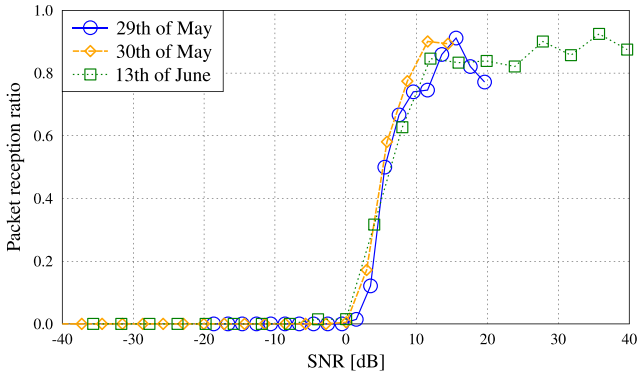

FIGURE 9. Estimated PRR versus SINR for 3 measurement campaigns on various days of the given month.

received. Data about the received packets are also correlated with our spectrum recordings, which were adjusted accordingly for the time and frequency offsets.

On the other hand, our base station is not capable of reliably estimating the SINR directly. Hence, to calculate SINR at the receiver side for each transmitted packet, we manipulate the recorded spectrum data accordingly. For each packet, the received signal strength, noise and interference power are required for the estimation. We achieved this estimation by summing up RSSI samples from the recorded spectrum data using two masks, one that covers only the signal transmission as illustrated on the left-hand side of Fig. 6, and the other that covers the immediate surroundings of the transmission as shown on the right-hand side of Fig. 6. We are able to realize this because the associated time duration and frequency bandwidth of the transmitted packets are known. Fig. 7 portrays these applied masks on real-time data for a single packet.

Assuming that the interference and noise power are constant during the addressed time-frequency window, the estimated power P_{total} using the first mask, so-called signal mask, includes signal power P_{sig}, interference power P_{int} and noise power P_{noise}, and is defined as follows:

$$P_{total} = P_{sig} + P_{int} + P_{noise}. \tag{18}$$

The estimated power P_{surr} using the second mask, so-called noise mask, includes only interference and noise power from the immediate surroundings, which can be defined by:

$$P_{surr} = P_{int} + P_{noise}. \tag{19}$$

By rearranging Eqs. (18) and (19), for each packet the received SINR can be estimated as follows:

$$SINR = \frac{P_{total} - P_{surr}}{P_{surr}}. \tag{20}$$

Relying on Eq. (20) and based on RSSI recordings, the linear dependence between the transmitter gain and SINR must be verified. Indeed, Fig. 8 advocates this linear dependency, which suggests that our SINR estimation method is reliable.

Consequently, we binned the packets according to their estimated SINR and acquired corresponding PRR value for each bin according to the packet loss data, which we obtained by comparing the packet sequence numbers. Fig. 9 represents the strict relationship between PRR and SINR obtained for 3 distinct measurement campaigns.

C. RESULT ANALYSES

Figs. 10, 11, 12 and 13 represent the performance of different channel metrics calculated for a recorded history of the 868 MHz band, where the frequency channel is placed on the horizontal axis and the availability of the proposed metric is provided on the vertical axis. All metrics have been calculated for a range of received powers levels P_{rx} [dBm],

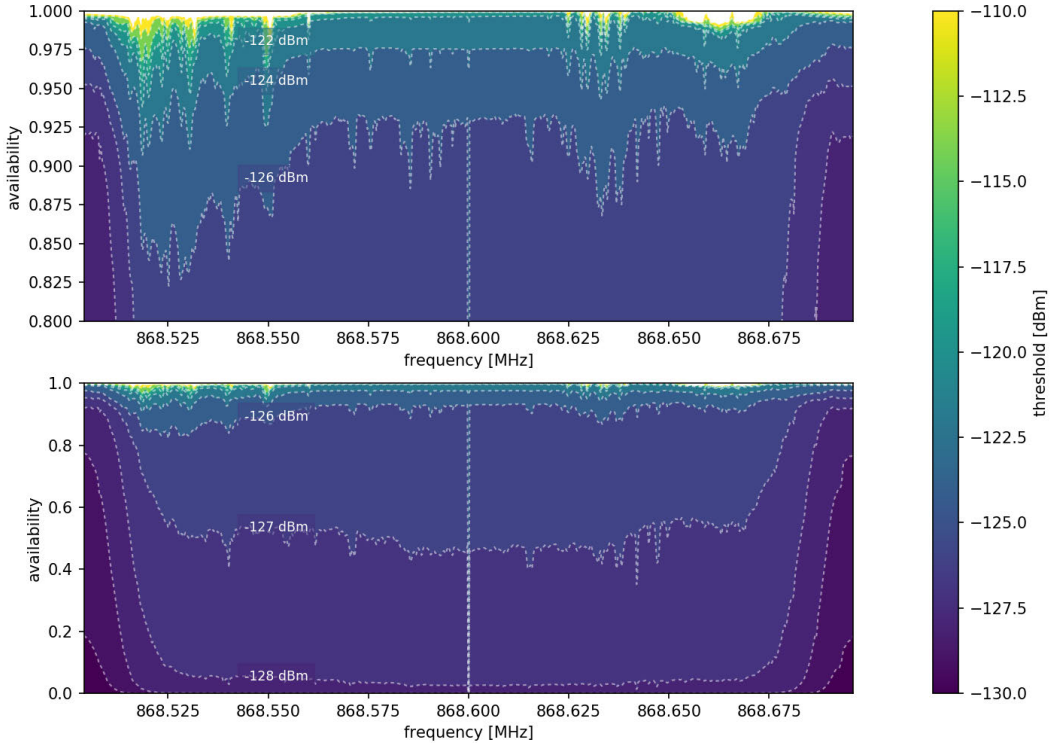

FIGURE 10. MCA metric.

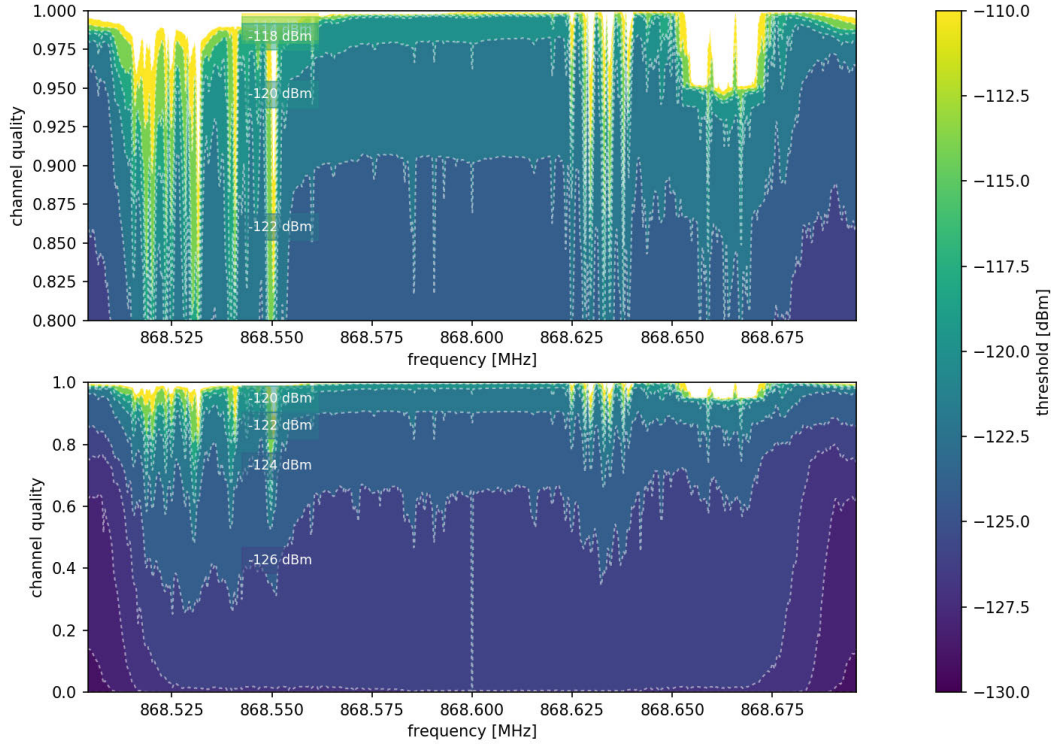

FIGURE 11. $CQ^*(\tau)$ metric.

which is represented on the color scale. In each of these figures, the bottom plots show the calculation over entire span of the received signal power, whereas the top plots represent a zoomed-in view of the vertical axis, where the channels with larger predicted PRR and higher channel availability can be readily observed.

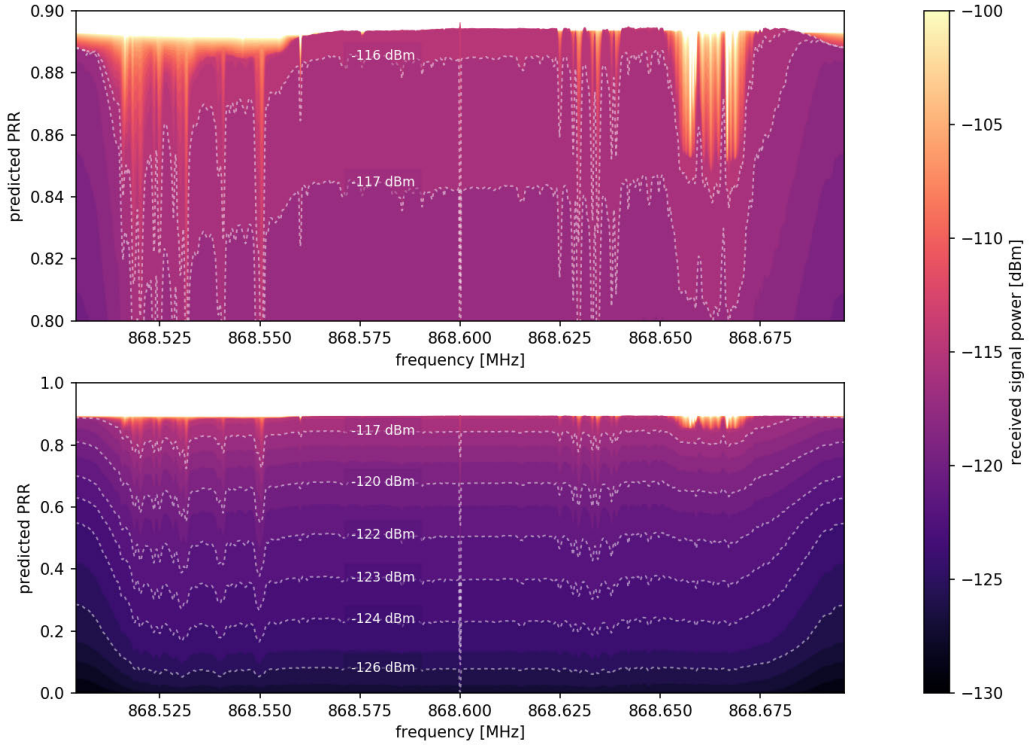

FIGURE 12. $\overline{PRR}$ **metric using measured** ***PRR*****(*****SINR*****).**

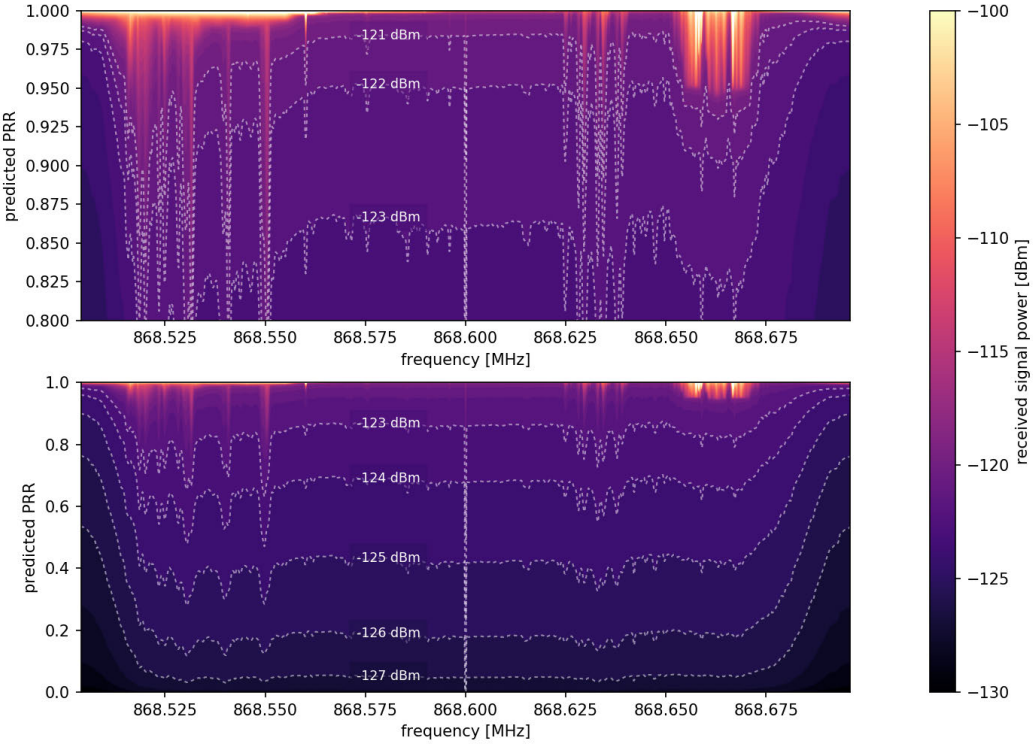

FIGURE 13. $\overline{PRR}$ **metric using theoretical** ***PRR*****(*****SINR*****).**

We now exploit estimated PRR in Eq. (17) using Eqs. (4) and (5), and data shown in Fig. 9 in order to simulate several scenarios and estimate the effect of whitelisting based on the measurements of the spectrum. Figs. 14 and 15 present the

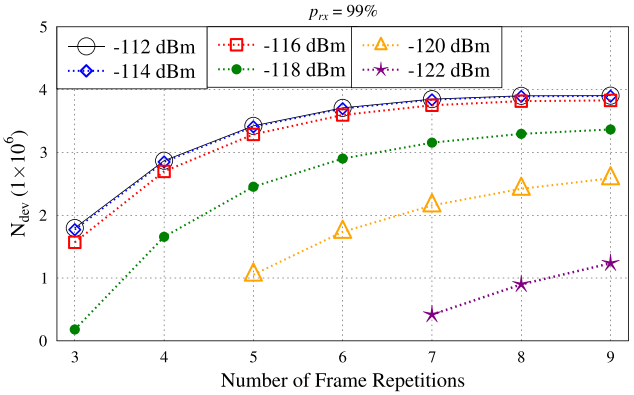

FIGURE 14. The average number of frame repetitions N_f required for the estimated maximum number of devices N_{dev} is presented for each received signal strength at the QoS requirement of a minimum probability of $p_{rx} = 0.99$.

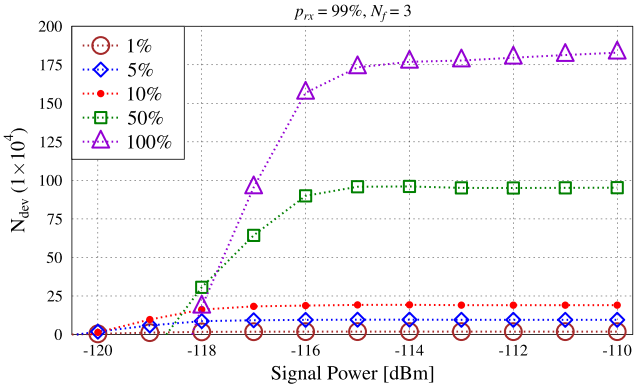

FIGURE 15. The average received signal power for the estimated maximum number of devices N_{dev} that the base station can support for the channel whitelisting percentage considered. Minimum probability of p_{rx} is 0.99 while devices transmit with $N_f = 3$ frame repetitions. Whitelisting is expressed as the percentage of all available channels, e.g. 1%, 5%, 10%, 50% and 100% of all available channels.

results of such a simulation from several perspectives. Noting that in all simulations, each device infrequently transmits data.

From Fig. 14, we can readily observe that reducing the number of frame repetitions decreases the capacity of the network and there is no clear optimum, especially for lower received signal power since the maximum achievable capacity has not converged. Conversely, for larger received signal power, the achievable capacity cannot be significantly improved beyond about 7 frame repetitions, which may suggest a near-optimal capacity solution. Besides, for a lower received signal power, higher number of retransmissions are required for an increased network capacity and the number of retransmissions cannot be reduced, which may be constrained by the QoS defined under certain channel conditions. Therefore, to satisfy such QoS requirements, whitelisting can be exploited so that relatively better channels can be utilized in order to attain lower number of retransmissions, while maintaining the anticipated capacity, as collaboratively demonstrated in Figs. 14 and 15.

Additionally in Fig. 15, the 100% line indicates that transmissions can benefit from all available channels without any whitelisting. At a chosen QoS (minimum p_{rx}), the number of devices that the network can support falls with the reduced received signal power. When the received signal power is around -120 dBm, the network can only support a few devices for various length of whitelist, such as 1%, 5% and 10%, and then N_{dev} falls to near '0' depending on the received signal power. If we compare the 100% line with the lines representing the reduced size of the whitelist, we can observe that the capacity of the network decreases with the smaller size of whitelist indicating that less degree of freedom induces capacity degradation. However, with the whitelist sizes smaller than 100%, there is a region between -122 dBm and -118 dBm, where the network can in fact support some devices at the chosen QoS, whereas this would have been impossible if all available channels were utilized. Therefore, channel whitelisting works well for supporting relatively lower received signal power transmissions. More explicitly, whitelisting would be beneficial for conserving more energy and increasing the overall reliability of the network, considering that the number of retransmissions required is reduced to 3 frames, as shown in Fig. 15 even for lower received signal power transmissions, which normally require larger number of retransmissions, as illustrated in Fig. 14.

VIII. DISCUSSIONS ON CHANNEL COHERENCE

In realistic environments the channel conditions dynamically change. This change determines the frequency of the update required for the whitelist. Contrarily, each downlink transmission of the whitelist to the devices incurs a certain cost in terms of downlink bandwidth and battery usage. Hence, the global knowledge of the whitelist should be distributed to each device as infrequent as possible. On the other hand, a whitelist that does not reflect the current channel state can significantly reduce the overall performance of the network. To alleviate this issue, we provide a discussion on the channel coherence with the analysis of stationarity and the coherence threshold.

To address the current channel states in the whitelist, we examine 28 days of empirical data and determine the *ad hoc* period during which the channels are assumed to remain in a consistent state, mainly described as the period, during which the whitelist is very likely to remain up-to-date. Then, the question can be reduced to how often should the base station broadcast the channel whitelist to be utilized by uplink transmissions.

If we presume that a time series of power spectra is an assembly of the stochastic processes, then the problem of channel coherence may be translated into a problem of determining the presence of stationarity in a stochastic process. Stationarity is a characteristic of a stochastic process, which signifies whether statistical moments of the process are time-invariant.

To test the stationarity and discover the length of temporal channel coherence, we employ a technique discussed

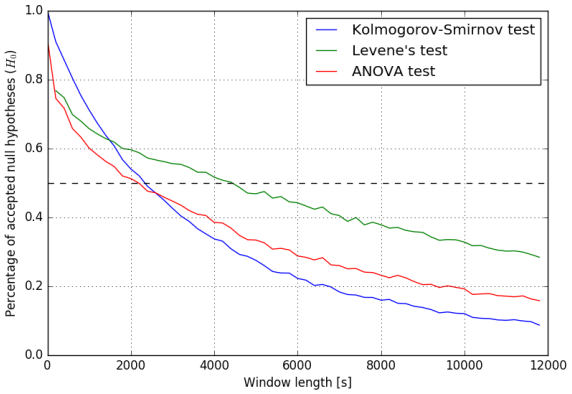

FIGURE 16. Average probability of stationarity (Kolmogorov-Smirnov, ANOVA and Levene's test) at $\alpha = 0.05$ for various time windows over all channels.

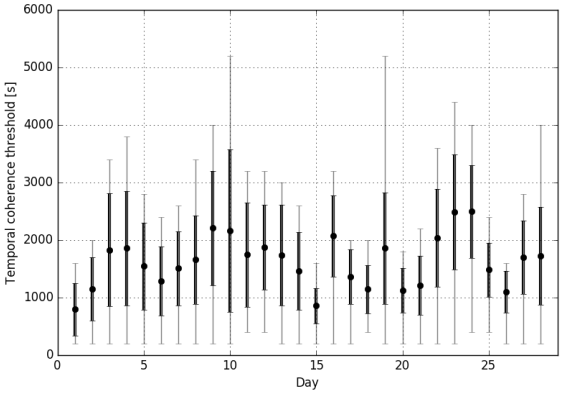

FIGURE 17. Channel temporal coherence threshold distribution (all channels) on various days, the standard deviation is bolded. The shortest time windows are excluded from analysis due to low accuracy of tests, caused by an insufficient number of data points in small time intervals.

in [32]. Initially, the spectrum data are partitioned into channels, where each channel is then split into a sequence of m non-overlapping intervals of length l. Independent hypothesis tests[6] for distribution fitting of data in addition to mean and variance stationarity tests are performed on each consecutive pair of intervals, totaling $m - 1$ pairwise comparisons per channel. Supposing that two consecutive intervals form a window of length $2l$ which is considered stationary if the null hypothesis on the corresponding intervals is satisfied. The probability of stationarity at length $2l$ is acquired by dividing the number of accepted null hypotheses by the total number of performed tests. The length of the intervals l is varied in order to obtain the probabilities of stationarity for different time windows.

A. TEMPORAL COHERENCE THRESHOLD

The results of our analysis are shown in Fig. 16. We define temporal coherence threshold as the shortest-longest period, during which the probability of stationarity remains above 50% for any test. The shortest period is used in order to ensure that our threshold is sensitive to changes in any tested characteristic of a channel, i.e. capturing a change in mean power and power variation as well as in power distribution.

The probability of stationarity is calculated for windows that were 100 seconds apart using all tests to capture any consecutive changes on our recorded data. For window length of approximately 37 minutes, the probability of 50% is attained for ANOVA test, indicating that the channel conditions have likely changed and the whitelists should be updated with current channel states, which can be accomplished from the base station. More explicitly, Fig. 16 demonstrates the average time duration until when the channels are on their unchanged state, with the assumption of 50% probability of stationarity and considering 28 days of data recordings. Therefore, considering the assumptions of the tests and 28 days of data recordings, it is safe to say that updating channels of whitelist after every 37 minutes highly likely guarantees to exploit relatively better channels for uplink transmissions.

[6]Kolmogorov-Smirnov, ANOVA and Levene's test.

Additionally, one way to ensure the up-to-date whitelist and to minimize the overheads incurred by the transmission of whitelists is to update channels of the whitelist just before the uplink transmissions are initiated, so that about 37 minutes time frame guarantees a highly likely unchanged whitelist for these uplink transmissions.

B. ON TEMPORAL AND SPATIAL COHERENCE STABILITY

The coherence threshold may fluctuate greatly with respect to both temporal and spatial variation, which is not only channel-dependent but also time-dependent, as illustrated in Fig. 17. For example, on the first day Fig. 17 suggests updating the channels after around 13 minutes so that a relatively up-to-date whitelist can be gleaned. Considering all channels for each day, the average coherence threshold has varied in order to obtain an up-to-date whitelist. For averaging these non-linear changes for 28 days, stationarity tests have been conducted in Fig. 16, which suggests that updating the channels every 37 minutes will highly likely ensure an up-to-date whitelist, taking into account the certain amount of data recordings and the assumptions made for the tests. Coherence time of the whole spectrum therefore cannot be characterized by one global model, but it can be analyzed independently for each channel or group of subchannels based on a certain amount of time period. Since updating whitelists at infinitely small or large intervals is impractical, determining the optimal coherence threshold and consequently whitelist retransmission time is dependent on the trade-offs. We have to maximize the retransmission time in order to minimize the number of whitelist retransmissions. Contrarily, minimization of the retransmission time is required for maximizing the number of channels that our coherence threshold is valid for. However, this trade-off is beyond the scope of our current study and will be considered as a future research direction.

IX. CONCLUSIONS AND FUTURE RESEARCH DIRECTIONS

In this paper we considered IoT frequency bands where intra- and inter-technology interference can influence the operation of existing protocol designs, such as the ones based

on RFDMA. We theoretically derived the conditions under which whitelisting can be beneficial in RFDMA networks and emprirically evaluated our findings. We derived an adaptive channel quality metric based on PRR as a function of the SINR that overcomes the shortcomings of other existing metrics, and through experimentation, we evaluated the proposed metric and demonstrated our theoretical findings.

Our theoretical findings are experimentally demonstrated on Sigfox, a particular type of RFDMA network. We showed that although channel whitelisting reduces the degree of freedom, and thus the overall capacity for received signal power levels larger than −118 dBm, it is readily observed that the achievable capacity is increased at a received signal power level below −118 dBm. This also enables a significant number of devices to be served at a much lower power level, which indicates the energy conservation capability of our whitelisting method. Moreover, it is shown that non-whitelisting scenarios are not capable of supporting any devices at a received signal power below −118 dBm. Additionally, even for lower received signal power levels, we are able to reduce the required number of retransmissions at the same reception probability, which indeed reveals an improved reliability for the network. It is readily evident that energy conservation and reliability in the UNB networks using RFDMA can be maintained by our channel whitelisting method.

Finding an optimal coherence threshold that can schedule whitelist retransmission is a potential future research direction to further improve our current work, as discussed at the end of Section VIII. Another improvement to our current study is to adopt the blacklisting (a dual concept to whitelisting) algorithm considered in [33] in order to minimize the computational overhead, since the generation of whitelists introduces a large computational overhead. Additionally, blacklisting/whitelisting can be extended to a distributed fashion [34] considering a negotiation between the transmitter and the receiver in order to create a blacklist/whitelist based on the PRR as a function of the SINR. Finally, integrating this study into a network that concerns message priorities should be an interesting way to improve the reliability and the capacity of the network. Then, for example, packets that carry the most important information can be only assigned to the best channels and the least important ones can be transmitted through moderately better channels depending on the QoS defined.

REFERENCES

[1] E. De Poorter, J. Hoebeke, M. Strobbe, I. Moerman, S. Latré, M. Weyn, B. Lannoo, and J. Famaey, "Sub-GHz LPWAN network coexistence, management and virtualization: An overview and open research challenges," *Wireless Pers. Commun.*, vol. 95, no. 1, pp. 187–213, Jul. 2017.

[2] R. Tavakoli, M. Nabi, T. Basten, and K. Goossens, "Enhanced time-slotted channel hopping in WSNs using non-intrusive channel-quality estimation," in *Proc. 12th IEEE Int. Conf. Mobile Ad Hoc Sensor Syst.*, Oct. 2015, pp. 217–225.

[3] K. Yang, N. Yang, N. Ye, M. Jia, Z. Gao, and R. Fan, "Non-orthogonal multiple access: Achieving sustainable future radio access," *IEEE Commun. Mag.*, vol. 57, no. 2, pp. 116–121, Feb. 2019.

[4] X. Gao, P. Wang, D. Niyato, K. Yang, and J. An, "Auction-based time scheduling for backscatter-aided RF-powered cognitive radio networks," *IEEE Trans. Wireless Commun.*, vol. 18, no. 3, pp. 1684–1697, Mar. 2019.

[5] A. M. Voicu, L. Simić, and M. Petrova, "Inter-technology coexistence in a spectrum commons: A case study of Wi-Fi and LTE in the 5-GHz unlicensed band," *IEEE J. Sel. Areas Commun.*, vol. 34, no. 11, pp. 3062–3077, Nov. 2016.

[6] T. Šolc, T. Gale, and C. Fortuna, "Optimization of ultra-narrowband wireless communication: An experimental case study," in *Proc. IEEE Conf. Comput. Commun. Workshops (INFOCOM WKSHPS)*, May 2017, pp. 523–528.

[7] H. Yetgin, K. T. K. Cheung, M. El-Hajjar, and L. H. Hanzo, "A survey of network lifetime maximization techniques in wireless sensor networks," *IEEE Commun. Surveys Tuts.*, vol. 19, no. 2, pp. 828–854, 2nd Quart., 2017.

[8] K. E. Nolan, W. Guibene, and M. Y. Kelly, "An evaluation of low power wide area network technologies for the Internet of Things," in *Proc. Int. Wireless Commun. Mobile Comput. Conf. (IWCMC)*, Paphos, Cyprus, Sep. 2016, pp. 439–444.

[9] M.-T. Do, C. Goursaud, and J.-M. Gorce, "Interference modelling and analysis of random FDMA scheme in ultra narrowband networks," in *Proc. Adv. Int. Conf. Telecommun. (AICT)*, Paris, France, Jul. 2014, pp. 132–137.

[10] M.-T. Do, C. Goursaud, and J.-M. Gorce, "On the benefits of random FDMA schemes in ultra narrow band networks," in *Proc. IEEE 12th Int. Symp. Modeling Optim. Mobile, Ad Hoc, Wireless Netw. (WiOpt)*, Hammamet, Tunisia, May 2014, pp. 672–677.

[11] N. Abramson, "The aloha system: Another alternative for computer communications," in *Proc. Fall Joint Comput. Conf.*, Nov. 1970, pp. 281–285.

[12] T. Šolc and C. Fortuna, "An adaptive channel quality metric for ultra-narrowband systems," in *Proc. Eur. Conf. Netw. Commun. (EuCNC)*, Jun. 2018, pp. 1–5.

[13] R. Ferrus, O. Sallent, and R. Agusti, "Interworking in heterogeneous wireless networks: Comprehensive framework and future trends," *IEEE Wireless Commun.*, vol. 17, no. 2, pp. 22–31, Apr. 2010.

[14] A. Lavric, A. I. Petrariu, and V. Popa, "Long range SigFox communication protocol scalability analysis under large-scale, high-density conditions," *IEEE Access*, vol. 7, pp. 35816–35825, Mar. 2019.

[15] A. Laya, C. Kalalas, F. Vazquez-Gallego, L. Alonso, and J. Alonso-Zarate, "Goodbye, ALOHA!" *IEEE Access*, vol. 4, pp. 2029–2044, 2016.

[16] G. Ferrari and O. K. Tonguz, "MAC protocols and transport capacity in ad hoc wireless networks: Aloha versus PR-CSMA," in *Proc. Military Commun. Conf. (MILCOM)*, Boston, MA, USA, vol. 2, Oct. 2003, pp. 1311–1318.

[17] Y. Mo, M.-T. Do, C. Goursaud, and J.-M. Gorce, "Optimization of the predefined number of replications in a ultra narrow band based IoT network," in *Proc. Wireless Days (WD)*, 2016, pp. 1–6.

[18] Y. Mo, M.-T. Do, C. Goursaud, and J.-M. Gorce, "Up-link capacity derivation for ultra-narrow-band IoT wireless networks," *Int. J. Wireless Inf. Netw.*, vol. 24, no. 3, pp. 300–316, 2017.

[19] T. Watteyne, A. Mehta, and K. Pister, "Reliability through frequency diversity: Why channel hopping makes sense," in *Proc. 6th ACM Symp. Perform. Eval. Wireless Ad Hoc, Sensor, Ubiquitous Netw.*, New York, NY, USA, Oct. 2009, pp. 116–123, doi: 10.1145/1641876.1641898.

[20] K. Jeon and S. Chung, "Adaptive channel quality estimation method for enhanced time slotted channel hopping on wireless sensor networks," in *Proc. 9th Int. Conf. Ubiquitous Future Netw. (ICUFN)*, Jul. 2017, pp. 438–443.

[21] V. Kotsiou, G. Z. Papadopoulos, P. Chatzimisios, and F. Theoleyre, "Whitelisting without collisions for centralized scheduling in wireless industrial networks," *IEEE Internet Things J.*, vol. 6, no. 3, pp. 5713–5721, Jun. 2019.

[22] C. Goursaud and Y. Mo, "Random unslotted time-frequency ALOHA: Theory and application to IoT UNB networks," in *Proc. 23rd Int. Conf. Telecommun. (ICT)*, May 2016, pp. 1–5.

[23] M. Vucnik, T. Solc, U. Gregorc, A. Hrovat, K. Bregar, M. Smolnikar, M. Mohorcic, and C. Fortuna, "Continuous integration in wireless technology development," *IEEE Commun. Mag.*, vol. 56, no. 12, pp. 74–81, Dec. 2018.

[24] V. Kotsiou, G. Z. Papadopoulos, D. Zorbas P. Chatzimisios, and A. F. Theoleyre, "Blacklisting-based channel hopping approaches in low-power and lossy networks," *IEEE Commun. Mag.*, vol. 57, no. 2, pp. 48–53, Feb. 2019.

[25] K. Balachandran, S. R. Kadaba, and S. Nanda, "Channel quality estimation and rate adaptation for cellular mobile radio," *IEEE J. Sel. Areas Commun.*, vol. 17, no. 7, pp. 1244–1256, Jul. 1999.
[26] D. Malone, P. Clifford, and D. J. Leith, "MAC layer channel quality measurement in 802.11," *IEEE Commun. Lett.*, vol. 11, no. 2, pp. 143–145, Feb. 2007.
[27] C. Noda, S. Prabh, M. Alves, C. A. Boano, and T. Voigt, "Quantifying the channel quality for interference-aware wireless sensor networks," *ACM SIGBED Rev.*, vol. 8, no. 4, pp. 43–48, Dec. 2011.
[28] X. Xing, T. Jing, Y. Huo, H. Li, and X. Cheng, "Channel quality prediction based on Bayesian inference in cognitive radio networks," in *Proc. IEEE INFOCOM*, Turin, Italy, Apr. 2013, pp. 1465–1473.
[29] V. Kotsiou, G. Z. Papadopoulos, P. Chatzimisios, and F. Tholeyre, "Is local blacklisting relevant in slow channel hopping low-power wireless networks?" in *Proc. IEEE Int. Conf. Commun. (ICC)*, May 2017, pp. 1–6.
[30] D. Gunatilaka, M. Sha, and C. Lu, "Impacts of channel selection on industrial wireless sensor-actuator networks," in *Proc. IEEE INFOCOM Conf. Comput. Commun.*, May 2017, pp. 1–9.
[31] T. Šolc, C. Fortuna, and M. Mohorčič, "Low-cost testbed development and its applications in cognitive radio prototyping," in *Cognitive Radio and Networking for Heterogeneous Wireless Networks*, A. F. Cattoni, L. De Nardis, J. Fiorina, F. Bader, and M. G. Di Benedetto, Eds. Cham, Switzerland: Springer, 2014, pp. 361–405.
[32] V. Chaganti, L. Hanlen, and D. Smith, "Are narrowband wireless on-body networks wide-sense stationary?" *IEEE Trans. Wireless Commun.*, vol. 13, no. 5, pp. 2432–2442, May 2014.
[33] C. Shih, A. E. Xhafa, and J. Zhou, "Practical frequency hopping sequence design for interference avoidance in 802.15.4e TSCH networks," in *Proc. IEEE Int. Conf. Commun. (ICC)*, London, U.K., Jun. 2015, pp. 6494–6499.
[34] P. H. Gomes, T. Watteyne, and B. Krishnamachari, "MABO-TSCH: Multihop and blacklist-based optimized time synchronized channel hopping," *Trans. Emerg. Telecommun. Technol.*, vol. 29, no. 7, p. e3223, Jul. 2018, doi: 10.1002/ett.3223.

TOMAŽ ŠOLC received the B.Sc. degree in electronics from the Faculty of Electrical Engineering, University of Ljubljana, in 2007. He is currently pursuing the Ph.D. degree with the Jožef Stefan International Postgraduate School. After spending four years in the industry as a Senior Software Engineer, he joined the Department of Communication Systems, Jožef Stefan Institute, as a Senior Research Assistant. His current research interests include hardware design, measurements and embedded software development, and research in the field of spectrum sensing. He participated in various national and EU projects involving advanced radio technologies, including H2020 eWINE, FP7 CREW, FP7 Fed4Fire, and the UK Ofcom TV White-space trials. In FP7 CREW, he was a Technical Lead in development of an out-door wireless testbed.

HALIL YETGIN received the B.Eng. degree in computer engineering from Selcuk University, Turkey, in 2008, the M.Sc. degree in wireless communications from the University of Southampton, U.K., in 2010, and the Ph.D. degree in wireless communications from the Next Generation Wireless Research Group, University of Southampton, in 2015. He is currently an Assistant Professor with the Department of Electrical and Electronics Engineering, Bitlis Eren University, Turkey, and a Research Fellow with the Department of Communication Systems, Jožef Stefan Institute, Ljubljana, Slovenia. His current research interests include the development of intelligent communication systems, energy efficient cross-layer design, resource allocation of the future wireless communication networks, UAV communication networks, and underwater sensor networks. He was a recipient of the full scholarship from the Republic of Turkey and Ministry of National Education.

TIMOTEJ GALE received the B.Sc. degree in computer and information science from the Faculty of Computer and Information Science, University of Ljubljana, in 2017, where he is currently pursuing the M.Sc. degree. He is currently a Student Researcher with the Department of Communication Systems, Jožef Stefan Institute, and a developer at multiple companies. His current research interests include application of data mining and machine learning methods, and concepts to a wide range of problems in telecommunication systems and networks with focus on data-driven technologies for the Internet of Things.

MIHAEL MOHORČIČ received the B.Sc., M.Sc., and Ph.D. degrees from the University of Ljubljana, Ljubljana, in 1994, 1998, and 2002, respectively, and the M.Phil. degree from the University of Bradford, Bradford, U.K., in 1998, all in electrical engineering. He is currently the Head of the Department of Communication Systems and a Scientific Counselor with the Jožef Stefan Institute, and an Associate Professor with the Jožef Stefan International Postgraduate School. He has authored or coauthored over 180 refereed journal and conference papers, coauthored three books, and contributed to nine book chapters. His current research interests include the development and performance evaluation of network protocols and architectures for mobile and wireless communication systems, and resource management in terrestrial, stratospheric, and satellite networks. His current research interests also include cognitive radio networks, smart applications of wireless sensor networks, dynamic composition of communication services, and wireless experimental testbeds. He has been participating as an editor-in-chief in many co-funded research projects, since 1996. He is currently involved in H2020 projects, including DEFENDER, Fed4FIRE+, NRG-5, SAAM, and RESILOC.

CAROLINA FORTUNA received the B.Sc. and Ph.D. degrees from IBCN, Ghent University, in 2006 and 2013, respectively. She was a Postdoctoral Research Associate with IBCN, Ghent University, from 2014 to 2015. She is currently a Research Fellow with the Department of Communication Systems, Jožef Stefan Institute and an Assistant with the Jožef Stefan International Postgraduate School. She coauthored over 50 peer-reviewed publications. Her current research interest includes interdisciplinary, focusing on data and knowledge driven modeling of communication and sensor systems. She has participated in H2020, FP7, and FP6 projects. In H2020 WiSHFUL, she was the Technical Leader of the project on behalf of UGhent/iMinds, while in FP7 CREW, she was the Technical Leader of the JSI Team. She was a TPC member with IEEE ICC 2011, 2012, 2013, 2014, 2016, ESWC 2012, IEEE GLOBECOM 2011, 2016, VTC 2010, 2016, and IEEE WCNC 2009, and gained industrial experience by working with Bloomberg LP and Siemens PSE.